




INFLUENCE OF ELECTRIC FIELD E_3 ON THE PHASE TRANSITION AND THERMODYNAMIC CHARACTERISTICS OF GPI FERROELECTRICS

R. R. Levitskii¹, I. R. Zachek², A. S. Andrushchak²

¹*Institute for Condensed Matter Physics of the National Academy of Sciences of Ukraine,
1, Svientsitskii St., Lviv, UA-79011, Ukraine*

²*Lviv Polytechnic National University, 12, Bandera St., Lviv, UA-79013, Ukraine*

(Received 22 February 2022; in final form 19 June 2022; accepted 04 July 2022; published online 10 September 2022)

Using the proposed model of the GPI ferroelectrics within the framework of the two-particle cluster approximation, the components of polarization vector and static dielectric permittivity tensor, piezoelectric characteristics, and molar specific heat of the crystal presence of the electric field E_3 are calculated. A possibility of appearance of the first order phase transition in the crystal is analyzed; the temperature and field behavior of the calculated thermodynamic characteristics are explored.

Key words: ferroelectrics, phase transition, dielectric permittivity, piezomoduli, electric field.

DOI: <https://doi.org/10.30970/jps.26.3601>

I. INTRODUCTION

One of the important problems in the physics of ferroelectric materials is the study of the effects that appear under the action of an external electric field. The field can be a powerful tool for a purposeful control of the materials' physical characteristics. The effects of the external fields depend both on the intensity and type of such an action and on the properties of the materials. The application of an electric field is a very important instrument for the investigation of ferroelectric materials with a complex spatial arrangement of the local effective dipole moments. As a result, these materials can undergo phase transitions with different but coupled order parameters. In particular, it appears possible to influence this system by means of an electric field, which is perpendicular to a spontaneous polarization, and to affect the polarization.

One of the most interesting examples of a crystal, sensitive to an electric field influence, is the glycinium phosphite (GPI), which belongs to ferroelectric materials with hydrogen bonds [1, 2]. At room temperature, this crystal has a monoclinic structure $P2_1/a$ [3]. The hydrogen bonds between the tetrahedra HPO_3 form infinite chains along the crystallographic c -axis. There are two types of hydrogen bonds: with the lengths $\sim 2.48 \text{ \AA}$ and $\sim 2.52 \text{ \AA}$ [3–5]. The ordering of protons on these bonds [4, 5] causes an antiparallel orientation of the components of dipole moments of the equivalent hydrogen bonds along the crystallographic axes a and c in the corresponding chains. On the other hand, the changes in some distances between ions in the HPO_3 tetrahedra and the corresponding components of the dipole moments of hydrogen bonds in the chains give rise to a net dipole moment along the b -axis. As a result, at 225 K the crystal undergoes a transition to the ferroelectric state (space group $P2_1$) with the spontaneous polarization perpendicular to the chains of

the hydrogen bonds. It should be noted that the phase transition in GPI is closely connected with the short- and long-range interactions within these chains and between them.

Highly important are the investigations of transverse electric fields' effects on the physical characteristics of GPI, as was discussed in detail in [10]. In [10–12] the influence of the transverse field E_3 on the phase transition and dielectric characteristics of GPI was explored. In [13] the thermodynamic characteristics of GPI for the E_3 field values between 0 and $\pm 4 \text{ MV/m}$ were evaluated; in [14], the calculated dielectric characteristics were used to show that the first order phase transition could emerge in GPI if the field E_3 exceeds the critical value $E_3^{\text{tr}} = 5.9 \text{ MV/m}$.

In the present paper, within the framework of the proposed model of a deformable GPI crystal, we explore the influence of the electric field E_3 on all its thermodynamic characteristics.

II. THERMODYNAMIC CHARACTERISTICS

The Hamiltonian of a proton subsystem of GPI, which takes into account the short-range and long-range interactions and the electric fields E_1 , E_2 , E_3 applied along positive directions of the Cartesian axes OX , OY and OZ , consists of the “seed” and pseudospin parts. The “seed” energy U_{pseed} corresponds to the heavy ion sublattice and does not depend explicitly on the configuration of the proton subsystem. The pseudospin part describes short-range \hat{H}_{short} and long-range \hat{H}_{MF} interactions of protons near the HPO_3 tetrahedra, as well as the effective interaction \hat{H}_{E} with the electric fields E_1 , E_2 , and E_3 . Therefore,

$$\hat{H} = NU_{\text{seed}} + \hat{H}_{\text{short}} + \hat{H}_{\text{MF}} + \hat{H}_{\text{E}}. \quad (1)$$

The U_{seed} corresponds to the “seed” energy, which includes the elastic, piezoelectric and dielectric parts:



$$\begin{aligned}
 NU_{\text{seed}} = Nv \left\{ \frac{1}{2} \sum_{i,i'=1}^3 c_{ii'}^{E0}(T) \varepsilon_i \varepsilon_{i'} + \frac{1}{2} \sum_{j=4}^6 c_{jj}^{E0}(T) \varepsilon_j^2 + \sum_{i=1}^3 c_{i5}^{E0}(T) \varepsilon_i \varepsilon_5 + c_{46}^{E0}(T) \varepsilon_4 \varepsilon_6 - \sum_{i=1}^3 e_{2i}^0 \varepsilon_i E_2 - e_{25}^0 \varepsilon_5 E_2 \right. \\
 \left. - e_{14}^0 \varepsilon_4 E_1 - e_{16}^0 \varepsilon_6 E_1 - e_{34}^0 \varepsilon_4 E_3 - e_{36}^0 \varepsilon_6 E_3 - \frac{1}{2} \chi_{11}^{\varepsilon 0} E_1^2 - \frac{1}{2} \chi_{22}^{\varepsilon 0} E_2^2 - \frac{1}{2} \chi_{33}^{\varepsilon 0} E_3^2 - \chi_{31}^{\varepsilon 0} E_3 E_1 \right\}, \quad (2)
 \end{aligned}$$

where N is the total number of the primitive cells of the Bravais lattice; v is the primitive cell volume. Parameters $c_{jj}^{E0}(T)$, e_{ij}^0 , $\chi_{ij}^{\varepsilon 0}$ are the so-called seed elastic constants, coefficients of piezoelectric voltage, and dielectric susceptibilities.

The Hamiltonian of short-range interactions is:

$$\hat{H}_{\text{short}} = -2w \sum_{qq'} \left(\frac{\sigma_{q1}}{2} \frac{\sigma_{q2}}{2} + \frac{\sigma_{q3}}{2} \frac{\sigma_{q4}}{2} \right) (\delta_{\mathbf{R}_q \mathbf{R}_{q'}} + \delta_{\mathbf{R}_q + \mathbf{R}_c, \mathbf{R}_{q'}}). \quad (3)$$

In \hat{H}_{short} σ_{qf} there is the z -component of the pseudospin operator corresponding to the f -th bond ($f = 1, 2, 3, 4$) in the q -th cell. The first and the second Kronecker deltas correspond to the interaction between protons in the chains near the HPO_3 tetrahedra of type ‘‘I’’ and type ‘‘II’’, respectively; \mathbf{R}_c is the lattice vector along the OZ -axis. Parameters w_1 , w_2 , which describe the short-range interactions within the chains, are expanded in the strains ε_j up to the linear terms

$$w_{1,2} = w^0 + \sum_l \delta_l \varepsilon_l \pm \delta_4 \varepsilon_4 \pm \delta_6 \varepsilon_6, \quad (l = 1, 2, 3, 5). \quad (4)$$

Mean field Hamiltonian \hat{H}_{MF} of the long-range dipole-dipole interactions and indirect (through the lattice vibrations) interactions between protons is as follows:

$$\begin{aligned}
 \hat{H}_{\text{MF}} = \frac{1}{2} \sum_{\substack{qq' \\ ff'}} J_{ff'}(qq') \frac{\langle \sigma_{qf} \rangle}{2} \frac{\langle \sigma_{q'f'} \rangle}{2} \\
 - \sum_{\substack{q'f' \\ ff'}} J_{ff'}(qq') \frac{\langle \sigma_{q'f'} \rangle}{2} \frac{\sigma_{qf}}{2}. \quad (5)
 \end{aligned}$$

Expanding the Fourier transforms of the interaction constants $J_{ff'} = \sum_{q'} J_{ff'}(qq')$ at $\mathbf{k} = 0$ in the strains ε_j up to the linear terms, we obtain

$$\begin{aligned}
 J_{33} &= J_{11}^0 + \sum_l \psi_{11l} \varepsilon_l \pm \psi_{114} \varepsilon_4 \pm \psi_{116} \varepsilon_6, \\
 J_{13} &= J_{13}^0 + \sum_l \psi_{13l} \varepsilon_l + \psi_{134} \varepsilon_4 + \psi_{136} \varepsilon_6, \\
 J_{34} &= J_{12}^0 + \sum_l \psi_{12l} \varepsilon_l \pm \psi_{124} \varepsilon_4 \pm \psi_{126} \varepsilon_6, \\
 J_{14} &= J_{23}^0 + \sum_l \psi_{14l} \varepsilon_l \pm \psi_{144} \varepsilon_4 \pm \psi_{146} \varepsilon_6, \\
 J_{22} &= J_{22}^0 + \sum_l \psi_{22l} \varepsilon_l \pm \psi_{224} \varepsilon_4 \pm \psi_{226} \varepsilon_6, \\
 J_{24} &= J_{24}^0 + \sum_l \psi_{24l} \varepsilon_l + \psi_{244} \varepsilon_4 + \psi_{246} \varepsilon_6.
 \end{aligned}$$

The term \hat{H}_{MF} can be written as

$$\hat{H}_{\text{MF}} = NH^0 - \sum_q \sum_{f=1}^4 \mathcal{H}_f \frac{\sigma_{qf}}{2}, \quad (6)$$

where

$$H^0 = \sum_{f,f'=1}^4 \frac{1}{8} J_{ff'} \eta_f \eta_{f'}, \quad \mathcal{H}_f = \sum_{f'=1}^4 \frac{1}{2} J_{ff'} \eta_{f'}, \quad \eta_f = \langle \sigma_{qf} \rangle. \quad (7)$$

The fourth term in (1) describes interactions of pseudospins with an external electric field:

$$\hat{H}_{\text{E}} = - \sum_{qf} \boldsymbol{\mu}_f \mathbf{E} \frac{\sigma_{qf}}{2}. \quad (8)$$

Here $\boldsymbol{\mu}_1 = (\mu_{13}^x, \mu_{13}^y, \mu_{13}^z)$, $\boldsymbol{\mu}_3 = (-\mu_{13}^x, \mu_{13}^y, -\mu_{13}^z)$, $\boldsymbol{\mu}_2 = (-\mu_{24}^x, -\mu_{24}^y, \mu_{24}^z)$, $\boldsymbol{\mu}_4 = (\mu_{24}^x, -\mu_{24}^y, -\mu_{24}^z)$ are the effective dipole moments per one pseudospin.

The two-particle cluster approximation (TPCA) is used for the calculation of thermodynamic and dielectric characteristics of GPI. In this approximation, the thermodynamic potential per one unit cell in the presence of stresses σ_j is given by:

$$\begin{aligned}
 g &= U_{\text{seed}} + H^0 - 2 \left(w^0 + \sum_l \delta_l \varepsilon_l \right) + 2k_{\text{B}} T \ln 2 \\
 &- Nv \sum_{i=1}^3 \sigma_i \varepsilon_i - \frac{1}{2} k_{\text{B}} T \sum_{f=1}^4 \ln(1 - \eta_f^2) - 2k_{\text{B}} T \ln D.
 \end{aligned}$$

Minimizing the thermodynamic potential, we obtain the system of equations for η_f and ε_j . Differentiating the equilibrium thermodynamic potential with respect to fields E_i , we obtain expressions for the polarization vector components P_i

$$\begin{aligned}
 P_1 &= e_{14}^0 \varepsilon_4 + e_{16}^0 \varepsilon_6 + \chi_{11}^{\varepsilon_0} E_1 + \frac{1}{2v} [\mu_{13}^x (\eta_1 - \eta_3) - \mu_{24}^x (\eta_2 - \eta_4)], \\
 P_2 &= e_{21}^0 \varepsilon_1 + e_{22}^0 \varepsilon_2 + e_{23}^0 \varepsilon_3 + e_{25}^0 \varepsilon_5 + \chi_{22}^{\varepsilon_0} E_2 + \frac{1}{2v} [\mu_{13}^y (\eta_1 + \eta_3) - \mu_{24}^y (\eta_2 + \eta_4)], \\
 P_3 &= e_{34}^0 \varepsilon_4 + e_{66}^0 \varepsilon_6 + \chi_{33}^{\varepsilon_0} E_3 + \frac{1}{2v} [\mu_{13}^z (\eta_1 - \eta_3) + \mu_{24}^z (\eta_2 - \eta_4)].
 \end{aligned} \tag{9}$$

Diagonal components of the static isothermal dielectric susceptibilities of mechanically clamped crystal GPI are given by:

$$\chi_{11}^{\varepsilon} = \left(\frac{\partial P_1}{\partial E_1} \right)_{\varepsilon_j} = \chi_{11}^{\varepsilon_0} + \frac{1}{2v\Delta} [\mu_{13}^x (\Delta_1^{\chi^a} - \Delta_3^{\chi^x}) - \mu_{24}^x (\Delta_2^{\chi^x} - \Delta_4^{\chi^x})], \tag{10}$$

$$\chi_{22}^{\varepsilon} = \left(\frac{\partial P_2}{\partial E_2} \right)_{\varepsilon_j} = \chi_{22}^{\varepsilon_0} + \frac{1}{2v\Delta} [\mu_{13}^y (\Delta_1^{\chi^y} + \Delta_3^{\chi^y}) - \mu_{24}^y (\Delta_2^{\chi^y} + \Delta_4^{\chi^y})], \tag{11}$$

$$\chi_{33}^{\varepsilon} = \left(\frac{\partial P_3}{\partial E_3} \right)_{\varepsilon_j} = \chi_{33}^{\varepsilon_0} + \frac{1}{2v\Delta} [\mu_{13}^z (\Delta_1^{\chi^z} - \Delta_3^{\chi^z}) + \mu_{24}^z (\Delta_2^{\chi^z} - \Delta_4^{\chi^z})]. \tag{12}$$

Here the ratio

$$\frac{\Delta_f^{\chi^\alpha}}{\Delta} = \left(\frac{\partial \eta_f}{\partial E_\alpha} \right)_{\varepsilon_l}$$

means the local pseudospin susceptibility, describing the response of the f -th order parameter to the external electric field E_α at constant strains.

From relations (9) we obtain the expressions for the isothermal coefficients of piezoelectric voltage e_{2l} of GPI

$$e_{1j} = \left(\frac{\partial P_1}{\partial \varepsilon_j} \right)_{E_1} = e_{1j}^0 + \frac{\mu_{13}^a}{2v\Delta} (\Delta_{1j}^e - \Delta_{3j}^e) - \frac{\mu_{24}^a}{2v\Delta} (\Delta_{2j}^e - \Delta_{4j}^e), (j = 4, 6), \tag{13}$$

$$e_{2l} = \left(\frac{\partial P_2}{\partial \varepsilon_l} \right)_{E_2} = e_{2l}^0 + \frac{\mu_{13}^b}{2v\Delta} (\Delta_{1l}^e + \Delta_{3l}^e) - \frac{\mu_{24}^b}{2v\Delta} (\Delta_{2l}^e + \Delta_{4l}^e), (l = 1, 2, 3, 5), \tag{14}$$

$$e_{3j} = \left(\frac{\partial P_3}{\partial \varepsilon_j} \right)_{E_3} = e_{3j}^0 + \frac{\mu_{13}^c}{2v\Delta} (\Delta_{1j}^e - \Delta_{3j}^e) + \frac{\mu_{24}^c}{2v\Delta} (\Delta_{2j}^e - \Delta_{4j}^e), (j = 4, 6). \tag{15}$$

Here the ratios

$$\frac{\Delta_{fl}^e}{\Delta} = \left(\frac{\partial \eta_f}{\partial \varepsilon_l} \right)_{E_2}, \quad \frac{\Delta_{fj}^e}{\Delta} = \left(\frac{\partial \eta_f}{\partial \varepsilon_j} \right)_{E_2}$$

describe the response of the f -th order parameter to strains $\varepsilon_l, \varepsilon_j$ at constant external fields.

Other dielectric, piezoelectric, and elastic characteristics of GPI can be obtained using the quantities found above.

The molar entropy and heat capacity of the proton subsystem are obtained by differentiating the thermodynamic potential with respect to temperature: $S = -N_A \left(\frac{\partial g}{\partial T} \right)_\sigma$, $\Delta C^\sigma = T \left(\frac{\partial S}{\partial T} \right)_\sigma$.

III. COMPARISON OF THE NUMERICAL CALCULATION RESULTS WITH EXPERIMENTAL DATA

To calculate the temperature and field dependences of dielectric and piezoelectric characteristics of GPI, we have to set the values of the following parameters: the parameters of short-range interactions w^0 ; the

parameters of long-range interactions $\nu_f^{0\pm}$ ($f=1,2,3$); deformational potentials δ_i , ψ_{fi}^\pm ($f=1,2,3$; $i=1, \dots, 6$); effective dipole moments μ_{13}^a ; μ_{24}^a ; μ_{13}^b ; μ_{24}^b ; μ_{13}^c ; μ_{24}^c ; the ‘‘seed’’ dielectric susceptibilities $\chi_{ij}^{\varepsilon_0}$, coefficients of piezoelectric stress e_{ij}^0 , and elastic constants c_{ij}^{E0} .

In order to determine these parameters, we use the experimental data for the temperature dependences of the following physical characteristics of GPI: $P_s(T)$ [16], ε_{11}^σ , ε_{33}^σ [1], d_{21} , d_{23} [18], and also the dependence of the phase transition temperature $T_c(p)$ [19] on hydrostatic pressure.

The primitive cell volume of GPI is $v_H = 0.601 \cdot 10^{-21} \text{ cm}^3$ [15].

Numerical analysis shows that thermodynamic characteristics depend on the two linear combinations of the long-range interaction parameters $\nu^{0+} = \nu_1^{0+} + 2\nu_2^{0+} + \nu_3^{0+}$ and $\nu^{0-} = \nu_1^{0-} + 2\nu_2^{0-} + \nu_3^{0-}$. The optimal values of these combinations are $\nu^{0+}/k_B = 10.57 \text{ K}$, $\nu^{0-}/k_B = -0.8 \text{ K}$; whereas for $\nu_f^{0\pm}$ we choose $\tilde{\nu}_1^{0+} = \tilde{\nu}_2^{0+} = \tilde{\nu}_3^{0+} = 2.643 \text{ K}$, $\tilde{\nu}_1^{0-} = \tilde{\nu}_2^{0-} = \tilde{\nu}_3^{0-} = 0.2 \text{ K}$, where $\tilde{\nu}_f^{0\pm} = \nu_f^{0\pm}/k_B$.

From the equation for the transition temperature $\Delta(T_c) = 0$ at given $\nu_1^{0+}, \nu_2^{0+}, \nu_3^{0+}$ we obtain the opti-

mal value of $w^0 = 820$ K. The optimal values of the deformation potentials are as follows: $\tilde{\delta}_1 = 500$ K, $\tilde{\delta}_2 = 600$ K, $\tilde{\delta}_3 = 500$ K, $\tilde{\delta}_4 = 150$ K, $\tilde{\delta}_5 = 100$ K, $\tilde{\delta}_6 = 150$ K; $\tilde{\delta}_i = \delta_i/k_B$.

Similarly, parameters ψ_{fi}^\pm enter the expressions for the thermodynamic quantities via the following 6 linear combinations $\psi_i^+ = \psi_{1i}^+ + 2\psi_{2i}^+ + \psi_{3i}^+$ and $\psi_i^- = \psi_{1i}^- + 2\psi_{2i}^- + \psi_{3i}^-$. The optimal values of ψ_{fi}^\pm are: $\tilde{\psi}_{f1}^+ = 87.9$ K, $\tilde{\psi}_{f2}^+ = 237.0$ K, $\tilde{\psi}_{f3}^+ = 103.8$ K, $\tilde{\psi}_{f4}^+ = 149.1$ K, $\tilde{\psi}_{f5}^+ = 21.3$ K, $\tilde{\psi}_{f6}^+ = 143.8$ K, $\tilde{\psi}_{fi}^- = 0$ K, where $\tilde{\psi}_{fi}^\pm = \psi_{fi}^\pm/k_B$.

The effective dipole moments in the paraelectric phase are $\boldsymbol{\mu}_{13} = (0.4, 4.02, 4.3) \cdot 10^{-18}$ esu-cm, $\boldsymbol{\mu}_{24} = (-2.3, -3.0, 2.2) \cdot 10^{-18}$ esu-cm. In the ferroelectric phase $\mu_{13}^y = 3.82 \cdot 10^{-18}$ esu-cm;

“Seed” coefficients of piezoelectric stress, dielectric susceptibilities and elastic constants are:

$$e_{21}^0 = e_{22}^0 = e_{23}^0 = e_{25}^0 = 0.0 \frac{\text{esu}}{\text{cm}^2}; \quad \chi_{11}^0 = 0.1, \quad \chi_{22}^0 = 0.403,$$

$$\chi_{33}^0 = 0.5, \quad \chi_{31}^0 = 0.0;$$

$$c_{11}^{0E} = 26.91 \cdot 10^{10} \frac{\text{dyn}}{\text{cm}^2}, \quad c_{12}^{0E} = 14.5 \cdot 10^{10} \frac{\text{dyn}}{\text{cm}^2},$$

$$c_{13}^{0E} = 11.64 \cdot 10^{10} \frac{\text{dyn}}{\text{cm}^2}, \quad c_{15}^{0E} = 3.91 \cdot 10^{10} \frac{\text{dyn}}{\text{cm}^2},$$

$$c_{22}^{0E} = (64.99 - 0.04(T - T_c)) \cdot 10^{10} \frac{\text{dyn}}{\text{cm}^2},$$

$$c_{23}^{0E} = 20.38 \cdot 10^{10} \frac{\text{dyn}}{\text{cm}^2},$$

$$c_{25}^{0E} = 5.64 \cdot 10^{10} \frac{\text{dyn}}{\text{cm}^2}, \quad c_{33}^{0E} = 24.41 \cdot 10^{10} \frac{\text{dyn}}{\text{cm}^2},$$

$$c_{35}^{0E} = -2.84 \cdot 10^{10} \frac{\text{dyn}}{\text{cm}^2}, \quad c_{55}^{0E} = 8.54 \cdot 10^{10} \frac{\text{dyn}}{\text{cm}^2},$$

$$c_{44}^{0E} = 15.31 \cdot 10^{10} \frac{\text{dyn}}{\text{cm}^2}, \quad c_{46}^{0E} = -1.1 \cdot 10^{10} \frac{\text{dyn}}{\text{cm}^2},$$

$$c_{66}^{0E} = 11.88 \cdot 10^{10} \frac{\text{dyn}}{\text{cm}^2}.$$

Now we shall discuss the temperature and E_3 field dependences of the physical characteristics of GPI obtained in the present paper.

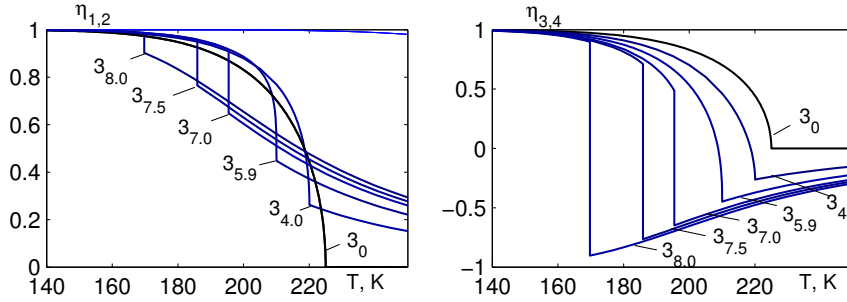


Fig. 1. The temperature dependences of the order parameters η_f of GPI at different values of electric field E_3 (MV/m), given by the lower index

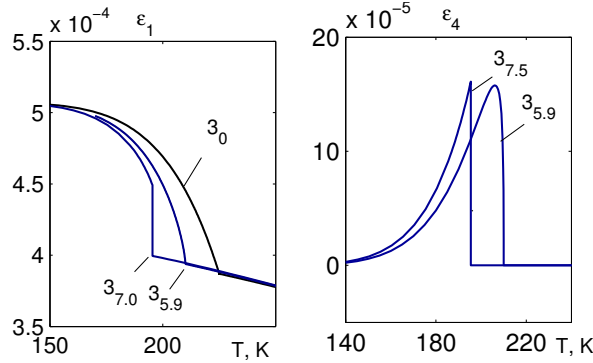


Fig. 2. The temperature dependences of strains $\varepsilon_1, \varepsilon_4$ of GPI at different values of the electric field E_3 (MV/m), given by the lower index

In the absence of an electric field, the following symmetry of the mean values of the pseudospins holds: $\eta_1 = \eta_3 = \eta_2 = \eta_4$ in the ferroelectric phase and $\eta_1 = \eta_2 = \eta_3 = \eta_4 = 0$ in the paraelectric phase (Fig. 1). The application of electric field E_3 leads to splitting of the pseudospin mean values, so that $\eta_1 = \eta_2 > 0$, $\eta_3 = \eta_4 < 0$ in the paraelectric phase. Increasing field E_3 in the paraelectric phase increases the order parameters η_1, η_2 and decreases η_3, η_4 . At the transition temperature T_c , the order parameters $\eta_1, \eta_2, \eta_3, \eta_4$ have jumps, if electric field E_3 is larger than a certain critical value

$E_3^{\text{tr}} = 5.9$ MV/m; with an increase in field E_3 , the jump magnitude decreases for η_1, η_2 and increases for η_3, η_4 .

Strains $\varepsilon_1, \varepsilon_2, \varepsilon_3, \varepsilon_5$ decrease with an increase in the field in the ferroelectric phase. If the field E_3 is above the critical one E_3^{tr} , these strains have jumps at T_c to their paraelectric phase values, which linearly decrease with an increase in temperature and do not depend on the field, as seen using the example of strain ε_1 , in Fig. 2. Strains $\varepsilon_4, \varepsilon_6$ increase with temperature in the ferroelectric phase, have maxima and downward jumps at $T = T_c$ (Fig. 2).

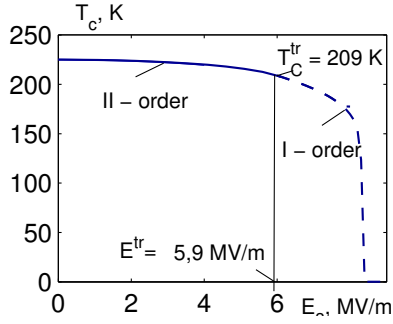


Fig. 3. The dependence of temperature T_c of the phase transition in GPI from the ferroelectric to the paraelectric phase on electric field $E_3(3)$.

In the ferroelectric phase with an increase in temperature the parameters of the short-range $w_{1,2}$ and long-range $\nu_{1,2,3}$ interaction parameters for GPI decrease along some convex curves down to their paraelectric phase values. When the field is above E_3^{tr} these parameters have jumps at T_c to their paraelectric phase values, which, in their turn, linearly decrease with

an increase in temperature and do not depend on the field.

The dependence of the phase transition temperature T_c of GPI on electric field E_3 is presented in Fig. 3. The transition temperature T_c decreases with field E_3 . At fields above the critical one $E_3^{\text{tr}} = 5.9$ MV/m (the tricritical point), the phase transition becomes of the first order (the dashed line).

In Fig. 4, the temperature dependences of polarization components P_i at different values of the field E_3 are shown.

In the absence of the field the spontaneous polarization monotonously and continuously decreases with an increase in temperature and vanishes at T_c (Fig. 4, curve 3₀₀). With increasing $|\Delta T|$, the magnitude of polarization P_2 increases and does not depend on the field at $E_3 < E_3^{\text{tr}}$ or increases with the field at $E_3 > E_3^{\text{tr}}$ (Fig. 5). At small fields E_3 the phase transition is of the second order. The temperature curves $P_2(T)$ are qualitatively similar to those at $E_3 = 0$ (Fig. 4, curves 3_{2,0}, 3_{4,0}). At fields above $E_3^{\text{tr}} \approx 5.9$ MV/m, the order of the phase transition changes to the first one, and the polarization $P_2(T)$ exhibits jumps at T_c , whose magnitudes increase with field E_3 (Fig. 4).

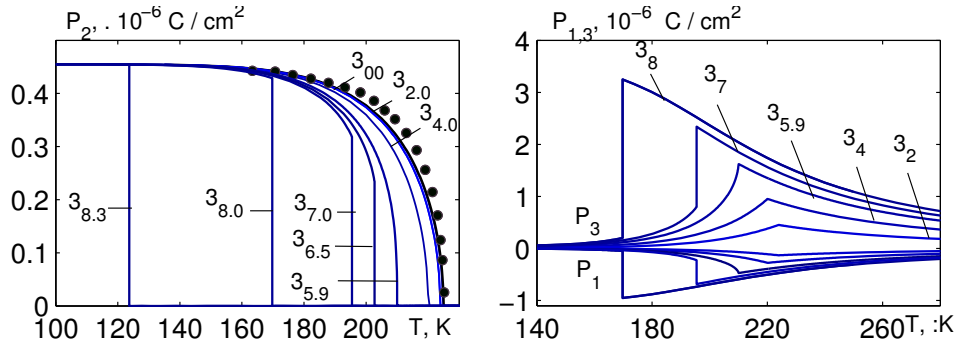


Fig. 4. The temperature dependences of polarizations P_2, P_1, P_3 of GPI at different values of field E_3 (MV/m), given by the lower index; $\circ - [16]$

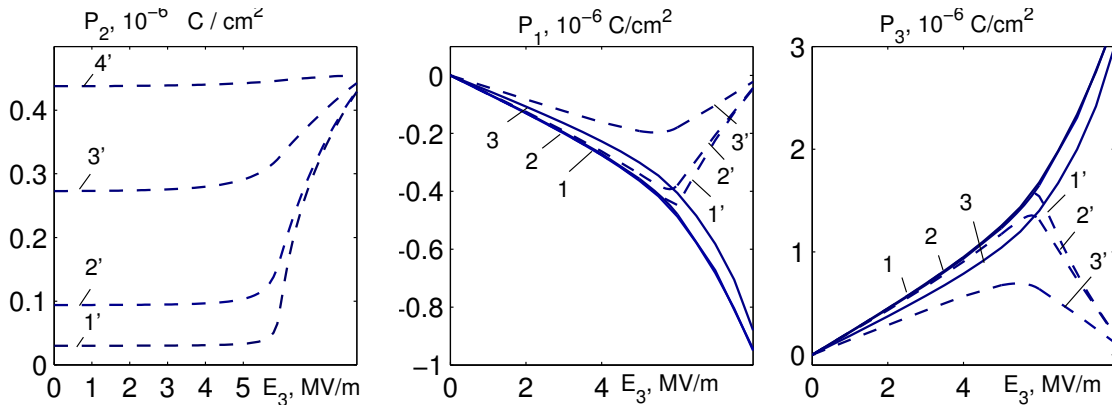


Fig. 5. Dependences of polarizations P_2, P_1, P_3 of GPI on field E_3 at different values of temperature ΔT (K): $-0.1 - 1'$; $-1.0 - 2'$; $-10.0 - 3'$; $-50.0 - 4'$; $0.1 - 1$; $1.0 - 2$; $10.0 - 3$

The transverse field E_3 also induces polarizations P_1 and P_3 , whose values are positive and negative, respectively (Fig. 4). At $E_3 < E_3^{\text{tr}}$, the temperature curves of $P_1(E_3)$ and $P_3(E_3)$ have cusps at T_c that transform into increasing with the field E_3 jumps at $E_3 > E_3^{\text{tr}}$ (Fig. 4). At $T > T_c$, field E_3 decreases $P_1(E_3)$ and increases $P_3(E_3)$. In the ferroelectric phase at $E_3 < E_3^{\text{tr}}$ the values of $P_1(E_3)$ decrease and of $P_3(E_3)$ increase with the field; at $E_3 > E_3^{\text{tr}}$ the values of $P_1(E_3)$ increase and of $P_3(E_3)$ decrease with an increase in the field.

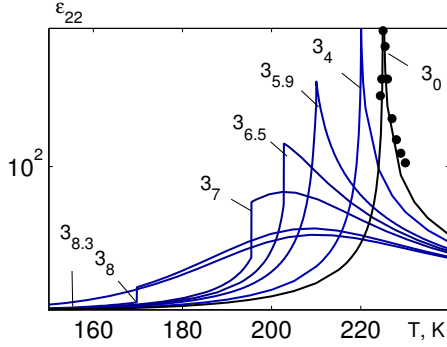


Fig. 6. The temperature dependences of static permittivity ε_{22} of GPI at different values of electric field E_3 (MV/m), given by the lower index. •: [17]

The changes in the temperature behavior of the static dielectric permittivities $\varepsilon_{22} = 1 + 4\pi\chi_{22}$ of GPI induced by the transverse electric field E_3 are shown in Fig. 6.

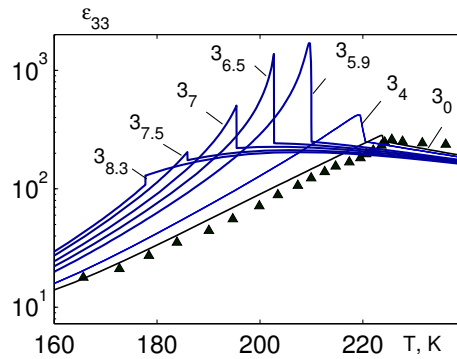
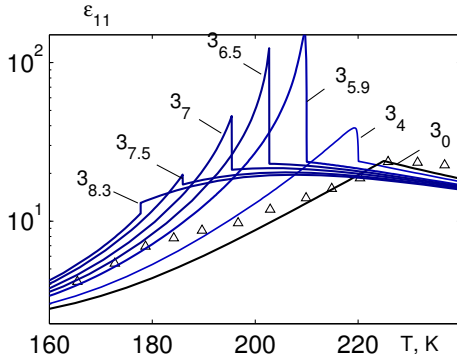


Fig. 8. The temperature dependences of static permittivities ε_{11} and ε_{33} of GPI at different values of electric field E_3 (MV/m), given by the lower index; ▲: [1].

The temperature curves of permittivities $\varepsilon_{11}(E_1)$, $\varepsilon_{33}(E_1)$ have a cusp at $T = T_c$ in the absence of the field (Fig. 8). The temperature curves of permittivities $\varepsilon_{11}(E_3)$ and $\varepsilon_{33}(E_3)$ exhibit jumps at the transition temperatures, which increase with an increase in field E_3 , are maximal at $E_3 = E_3^{\text{tr}}$, and shift to lower temperatures (Fig. 9). At $E_3 > E_3^{\text{tr}}$, the jumps of permittivities $\varepsilon_{11}(E_1)$, $\varepsilon_{33}(E_1)$ at $T = T_c$ decrease.

The temperature dependences of coefficients $e_{21}(T)$ and constants $h_{21}(T)$ of piezoelectric voltage at different values of electric field E_3 are shown in Fig. 10. At $E_3 = 0$, coefficient $e_{21}(T)$ diverges at T_c . When field E_3 is applied, coefficient $e_{21}(T)$ remains finite and jumps to zero at the transition to the paraelectric phase; the jump values

If the transverse field is below the critical one $E_3 < E_3^{\text{tr}}$, the longitudinal dielectric permittivity of a free crystal ε_{22} diverges at T_c . At $E_3 > E_3^{\text{tr}}$, when the phase transition becomes of the first order, the permittivity ε_{22} remains finite, and its maximal values decrease with an increase in the field. At $T = T_c$, the permittivity ε_{22} has a jump, whose magnitude decreases with an increase in field E_3 .

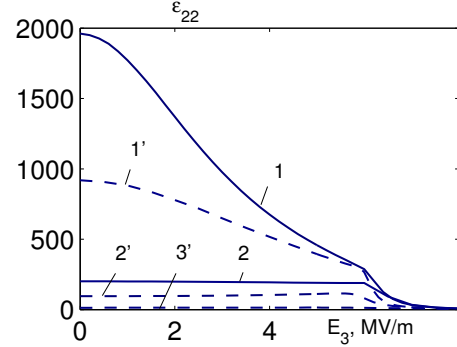


Fig. 7. Dependences of the static permittivity ε_{22} of GPI on electric field E_3 at different values of temperature T (K): $-0.1 - 1'$; $-1.0 - 2'$; $-10.0 - 3'$; $0.1 - 1$; $1.0 - 2$

The dielectric permittivity $\varepsilon_{22}(E_3)$ decreases with increasing field E_3 in the vicinity of the transition temperature ($\Delta T = \pm 0.1$ K), is field independent at larger $|\Delta T|$, if the field is below the critical one $E_3 < E_3^{\text{tr}}$, and decreases at $E_3 > E_3^{\text{tr}}$ (Fig. 7).

decrease with an increase in E_3 .

At $E_3 < E_3^{\text{tr}}$ and $\Delta T = 0.1$ K, the coefficient $e_{21}(E_3)$ first decreases and then increases up to a maximum at $E_3 = E_3^{\text{tr}}$. At larger ΔT , the values of $e_{21}(E_3)$ slightly increase with the field at $E_3 < E_3^{\text{tr}}$, are maximal at $E_3 = E_3^{\text{tr}}$, and decrease at $E_3 > E_3^{\text{tr}}$ with increasing ΔT (Fig. 11).

The constants of piezoelectric voltage $h_{21}(3)$ at different ΔT slightly increase with the field at $E_3 < E_3^{\text{tr}}$, then have a maximum as E_3 approaches E_3^{tr} ; the larger ΔT , the higher are the maximal values of $h_{21}(3)$. With further increase in the field, the constants $h_{21}(3)$ decrease (Fig. 11).

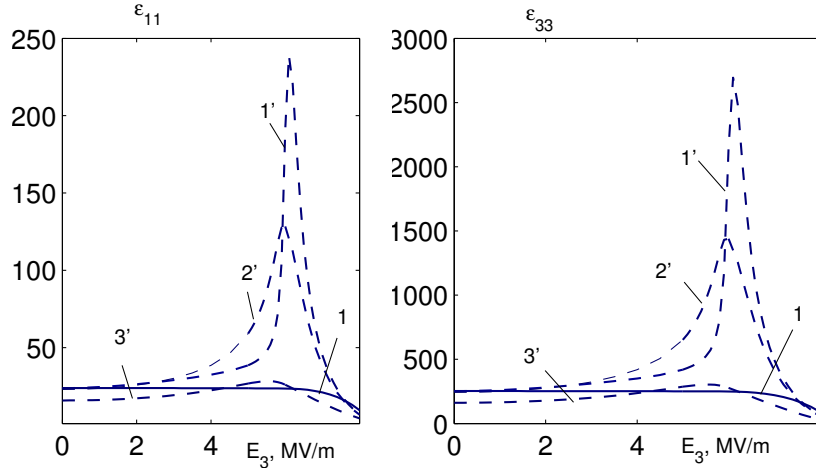


Fig. 9. Dependences of static permittivities ε_{11} and ε_{33} of GPI on electric field E_3 at different values of temperature ΔT (K): $-0.1 - 1'$; $-1.0 - 2'$; $-10.0 - 3'$; $0.1 - 1$

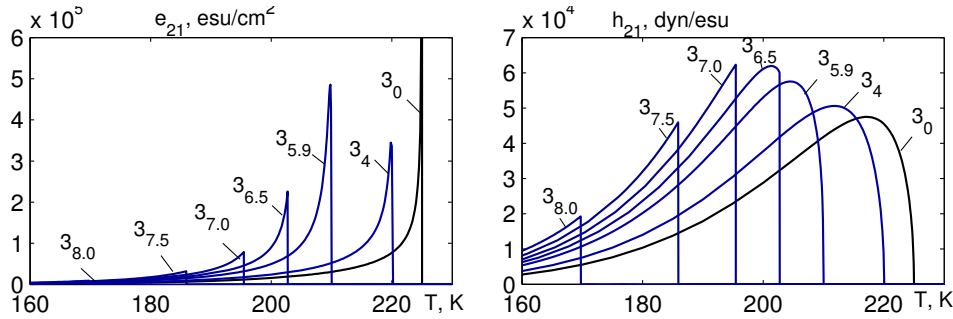


Fig. 10. The temperature dependences of coefficients $e_{21}(T)$ and constants $h_{21}(T)$ of piezoelectric voltage at different values of GPI at different values of electric field E_3 (MV/m), given by the lower index

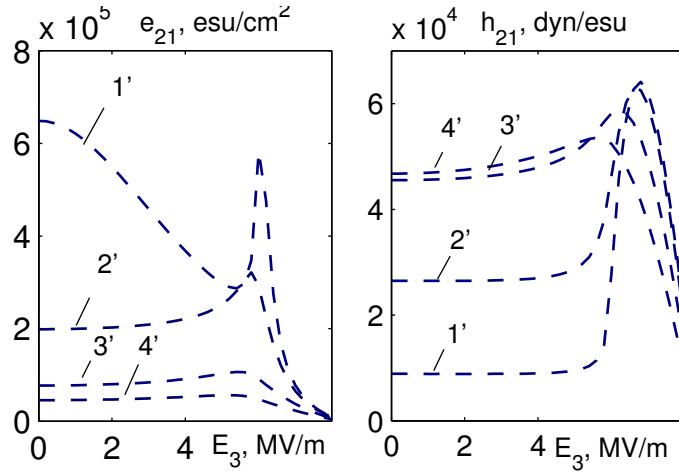


Fig. 11. Dependences of coefficient e_{14} and constant h_{14} of the piezoelectric voltage of GPI_{0.2}DGPI_{0.8} on electric field E_3 at different temperatures ΔT (K): $-0.1 - 1'$; $-1.0 - 2'$; $-5.0 - 3'$; $-10.0 - 4'$

The temperature dependences of coefficients $e_{14}(T)$ and $e_{34}(T)$ and constants $h_{14}(T)$, $h_{34}(T)$ of piezoelectric voltage of GPI at different values of electric field E_3 are presented in Fig. 12.

With an increase in field E_3 the absolute values of coefficients $e_{14}(E_3)$, $|e_{34}(E_3)|$ and constants $h_{14}(E_3)$, $|h_{34}(E_3)|$ of piezoelectric voltage increase, reaching their maxima at $E_3 = E_3^{\text{tr}}$, and then decrease; the larger

ΔT , the smaller the maximal values of these piezomoduli (Fig. 13).

The influence of field E_3 on the proton contribution to the molar specific heat at constant pressure ΔC_p is related mostly to the decrease in T_c and is revealed as a decrease in the maximal value of $\Delta C_p(E_3)$ at the transition temperature with an increase in the transverse electric field (Fig. 14).

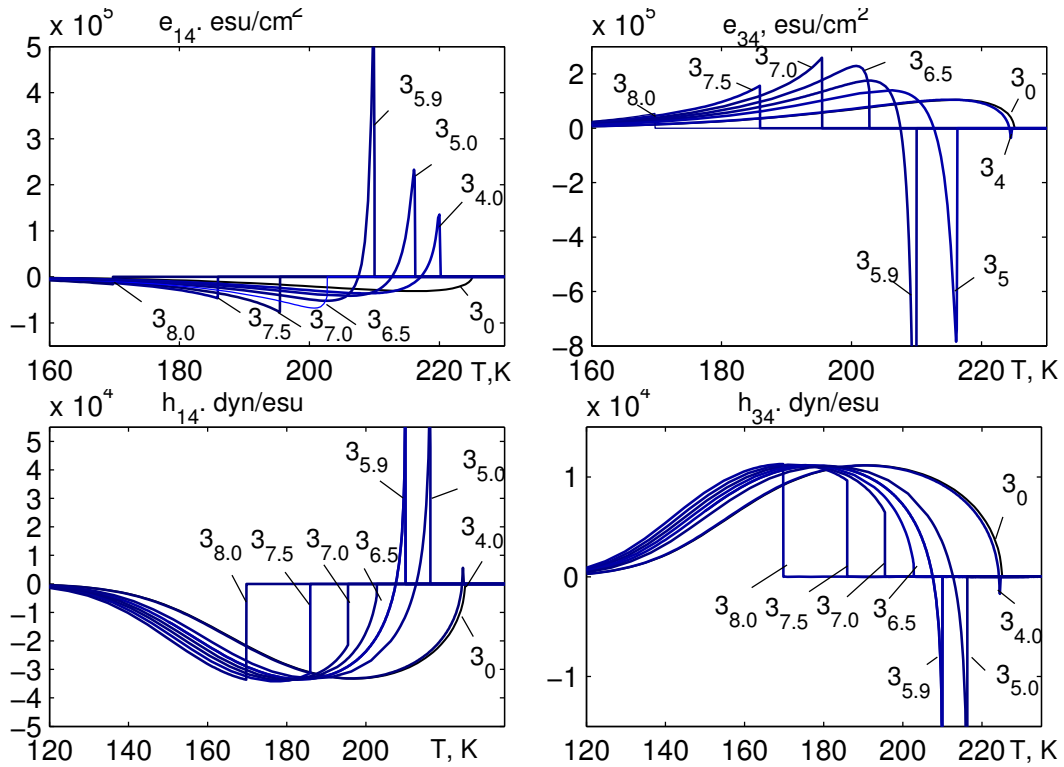


Fig. 12. The temperature dependences of coefficients $e_{14}(T)$ and $e_{34}(T)$ and constants $h_{14}(T)$, $h_{34}(T)$ of piezoelectric voltage of GPI at different values of electric field E_3 (MV/m), given by the lower index

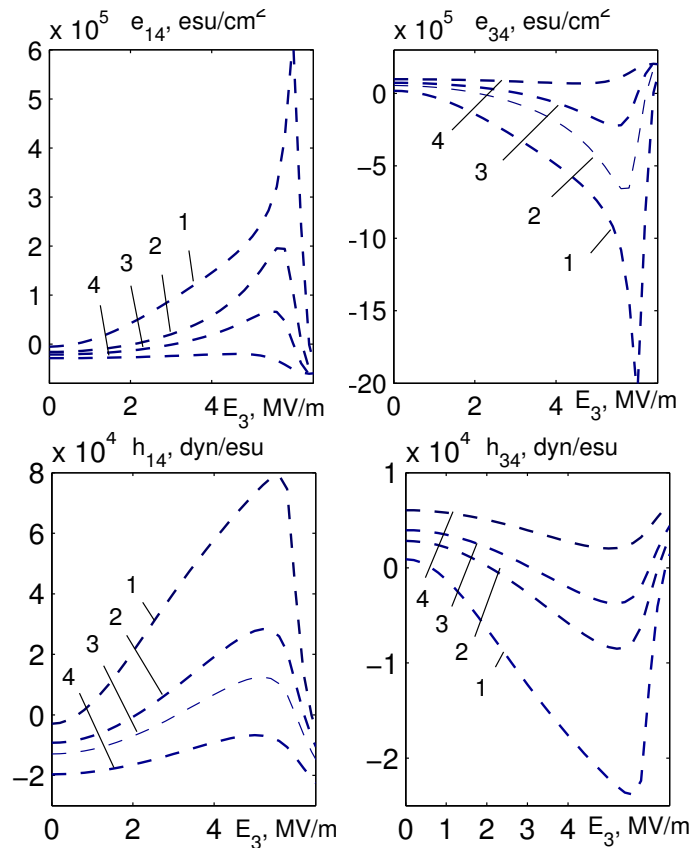


Fig. 13. Dependences of coefficients e_{14} , e_{34} and constants h_{14} , h_{34} of piezoelectric voltage of GPI on electric field E_3 at different values of temperature ΔT , (K): $-0.1 - 1$; $-1.0 - 2$; $-2.0 - 3$; $-5.0 - 4$

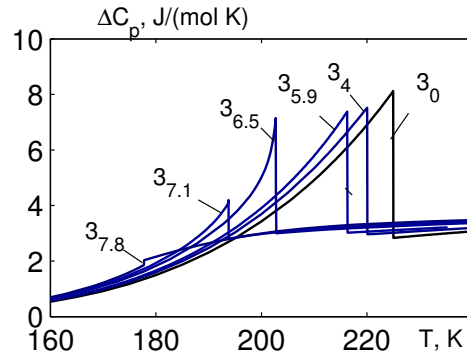


Fig. 14. The temperature dependence of the proton contribution to the molar specific heat ΔC_p of GPI at different values of electric field E_3 (MV/m), given by the lower index

IV. CONCLUSIONS

Using the proposed model of a deformed GPI crystal, we calculate its thermodynamic characteristics in the presence of electric field E_3 . The transition temperature $T_c(E_3)$ decreases with a decrease in field E_3 . At fields

above the critical one $E_3^{\text{tr}} = 5.9$ MV/m (the tricritical point), the phase transition is of the first order. Electric field E_3 induces polarizations P_1 and P_3 , whose temperature dependences are analyzed in the present paper. All thermodynamic characteristics at fields above the critical one have jumps at $T = T_c$.

-
- [1] S. Dacko, Z. Czapla, J. Baran, M. Drozd, *Phys. Lett. A* **221**, 217 (1996); [https://doi.org/10.1016/S0375-9601\(96\)00698-6](https://doi.org/10.1016/S0375-9601(96)00698-6).
- [2] J. Baran, G. Bator, R. Jakubas, M. Śledź, *J. Phys. Condens. Matter* **8**, 10647 (1996); <https://doi.org/10.1088/0953-8984/8/49/049>.
- [3] M.-T. Averbuch-Pouchot, *Acta Crystallogr. C* **49**, 815 (1993); <https://doi.org/10.1107/S0108270192010771>.
- [4] F. Shikanai, M. Komukae, Z. Czapla, T. Osaka, *J. Phys. Soc. Jpn.* **71**, 498 (2002); <https://doi.org/10.1143/JPSJ.71.498>.
- [5] H. Taniguchi, M. Machida, N. Koyano, *J. Phys. Soc. Jpn.* **72**, 1111 (2003); <https://doi.org/10.1143/JPSJ.72.1111>.
- [6] J. Baran, M. Śledź, R. Jakubas, G. Bator, *Phys. Rev. B* **55**, 169 (1997); <https://doi.org/10.1103/PhysRevB.55.169>.
- [7] R. Tchukvinskyi *et al.*, *Acta Phys. Pol. A* **92**, 1191 (1997); <https://doi.org/10.12693/APhysPolA.92.1191>.
- [8] R. Sobiestianskas, A. Brilingas, Z. Czapla, *J. Korean Phys. Soc.* **32**, 377 (1998).
- [9] J. Furtak, Z. Czapla, A. V. Kityk, *Z. Naturforsch.* **52a**, 778 (1997); <https://doi.org/10.1515/zna-1997-1104>.
- [10] I. V. Stasyuk, R. R. Levitskii, A. P. Moina, A. G. Slivka, O. V. Velychko *Field and Deformational Effects in Complex Ferroelectric Compounds* (Grazhda, Uzhgorod, 2009).
- [11] I. Stasyuk, Z. Czapla, S. Dacko, O. Velychko, *J. Phys. Condens. Matter* **16**, 1963 (2004); <https://doi.org/10.1088/0953-8984/16/12/006>.
- [12] I. Stasyuk, O. Velychko, *Ferroelectrics* **300**, 121 (2004); <https://doi.org/10.1080/00150190490443622>.
- [13] A. S. Vdovych, I. R. Zachek, R. R. Levitskii, I. V. Stasyuk, *Phase Transit.* **92**, 430 (2019); <https://doi.org/10.1080/01411594.2019.1590831>.
- [14] A. S. Vdovych, *Ukr. J. Phys.* **66**, 412 (2021); <https://doi.org/10.15407/ujpe66.5.412>.
- [15] F. Shikanai, M. Yamasaki, M. Komukae, T. Osaka, *J. Phys. Soc. Jpn.* **72**, 325 (2003); <https://doi.org/10.1143/JPSJ.72.325>.
- [16] J. Nayeem *et al.*, *Ferroelectrics* **332**, 13 (2006); <https://doi.org/10.1080/00150190500309064>.
- [17] J. Nayeem, H. Wakabayashi, T. Kikuta, T. Yamazaki, N. Nakatani, *Ferroelectrics* **269**, 153 (2002); <https://doi.org/10.1080/713716051>.
- [18] M. Wiesner, *Phys. Status Solidi (b)* **238**, 68 (2003); <https://doi.org/10.1002/pssb.200301750>.
- [19] N. Yasuda, T. Sakurai, Z. Czapla, *J. Phys. Condens. Matter* **9**, L347 (1997); <https://doi.org/10.1088/0953-8984/9/23/003>.

**ВПЛИВ ЕЛЕКТРИЧНОГО ПОЛЯ E_3 НА ФАЗОВИЙ ПЕРЕХІД І ТЕРМОДИНАМІЧНІ
ХАРАКТЕРИСТИКИ СЕГНЕТОЕЛЕКТРИКА GPI**

Р. Р. Левицький¹, І. Р. Зачек², А. С. Андрущак²

¹ *Інститут фізики конденсованих систем НАН України, вул. Свенціцького, 1, Львів, 79011, Україна*

² *Національний університет "Львівська політехніка", вул. С. Бандери, 12, Львів, 79013, Україна*

Одним із найцікавіших прикладів кристала, чутливого до впливу електричного поля, є фосфіт гліцину (glycine phosphite – GPI), що належить до сегнетоактивних матеріалів із водневими зв'язками. За кімнатної температури цей кристал має моноклінну структуру (просторова група $P2_1/a$). Водневі зв'язки між тетраедрами HPO_3 утворюють безмежні ланцюжки вздовж кристалографічної осі c . Розрізняють два типи водневих зв'язків: довжиною $\sim 2.48 \text{ \AA}$ і $\sim 2.52 \text{ \AA}$. Фазовий перехід у GPI тісно пов'язаний з коротко- та далекосяжними взаємодіями в цих ланцюжках і між ними.

Використовуючи запропоновану модель сегнеоелектрика GPI в наближення двочастинкового кластера, розраховано компоненти вектора поляризації та тензора статичної діелектричної проникності, п'єзоелектричні характеристики та молярну теплоємність кристала під час прикладання електричного поля E_3 . Зі зростанням поля E_3 температура фазового переходу T_c знижується. За полів, сильніших, ніж деяке критичне $E_3^{\text{tr}} = 5.9 \text{ МВ/м}$ (трикритична точка), фазовий перехід стає переходом першого роду. За полів, сильніших, ніж $E_3^{\text{tr}} \approx 5.9 \text{ МВ/м}$, поляризація $P_2(T)$ має стрибки в точці T_c , величини яких зі збільшенням поля E_3 зростають. За полів $E_3 < E_3^{\text{tr}}$ у температурному ході криві $P_1(E_3)$ і $P_3(E_3)$ мають злам у точці T_c , а за $E_3 > E_3^{\text{tr}}$ компоненти $P_1(E_3)$ і $P_3(E_3)$ мають стрибки в точці T_c , які зростають із збільшенням напруженості поля E_3 . В околі температури переходу ($\Delta T = \pm 0.1 \text{ К}$) зі збільшенням напруженості поля E_3 діелектрична проникність $\varepsilon_{22}(E_3)$ зменшується, за більших $|\Delta T|$ до величини поля $E_3 < E_3^{\text{tr}}$ від поля не залежить, а за $E_3 > E_3^{\text{tr}}$ — зменшується. У температурному ході проникностей $\varepsilon_{11}(E_3)$ і $\varepsilon_{33}(E_3)$ за температур фазових переходів спостерігаються стрибкоподібні зміни цих величин, які збільшуються зі зростанням напруженості поля E_3 , досягаючи максимуму за $E_3 = E_3^{\text{tr}}$, і зміщуються в бік нижчих температур. За напруженостей $E_3 > E_3^{\text{tr}}$ величина скачка проникностей $\varepsilon_{11}(E_1)$, $\varepsilon_{33}(E_1)$ за $T = T_c$ зменшується.

Під час прикладання поля E_3 коефіцієнти $e_{21}(T)$ стають скінченними, за температур $T = T_c$ вони скачкоподібно змінюються до нуля в парафазі й величина скачка зменшується зі зростанням поля E_3 . Вплив поля E_3 на протонний внесок у молярну теплоємність за сталого тиску ΔC_p проявляється в зменшенні максимального значення $\Delta C_p(E_3)$ за температури фазового переходу зі збільшенням напруженості поперечного електричного поля.

Ключові слова: сегнеоелектрики, фазовий перехід, діелектрична проникність, п'єзомодулі, електричне поле.